

Femtosecond control of magneto-optical effects in magnetoplasmonic crystals

A.V. Chetvertukhin, M.R. Shcherbakov, P.P. Vabishchevich, A.Yu. Frolov,
T.V. Dolgova, M. Inoue^a, and A.A. Fedyanin

Faculty of Physics, Lomonosov Moscow State University, Moscow 119991, Russia

^aToyohashi University of Technology, Toyohashi 441-8580, Japan

ABSTRACT

We have demonstrated remarkable enhancement of longitudinal and transverse magneto-optical Kerr effects in magnetoplasmonic crystals based on thin nanostructured films of nickel and iron due to resonant excitation of magnetoplasmonic waves in Faraday and Voigt configurations. Manifestations of ultrafast time-dependent transverse magneto-optical Kerr effect are experimentally demonstrated in femtosecond laser pulses reflected from a one-dimensional magnetoplasmonic crystal. We show that exciting surface plasmon-polaritons with magnetization-dependent dispersion law allows one to control the shape of the reflected pulse.

Keywords: Nanoplasmonics, magnetoplasmonics, ultrafast processes

1. INTRODUCTION

Plasmonics is one of the rapidly developing areas of modern photonics, particularly because of the fact that the frequency and nature of the propagation of a surface plasmon on a metal surface can be determined by a variety of external influences including magnetic field application,¹⁻⁴ as well as by the structuring the surface.⁵ New technological means of surface processing make nanoscale plasmonics a hot topic again. If a surface plasmon-polariton (SPP) propagates along a perforated metal surface, the conditions of its excitation, scattering and dispersion relations are substantially modified and even can be tailored by nanostructuring parameters.^{6,7} The SPP excitation is possible in a wide spectral range and at the different angles of incidence without extra elements such as prisms. Fano resonances appear in the spectral range of SPP excitation where SPP lifetime changes significantly due to the strong spectral dependence of the radiative losses. A special case of a perforated metal surface is a structure with a period close to the wavelength of light that excites the surface plasmons, called plasmonic crystals, as it can form a bandgap for SPPs. If the frequency of the SPP is close to the plasmon band gap, its' dispersion varies considerably, leading to features in the optical response of such media.⁸

Surface plasmon propagating on a magnetized surface or in an external magnetic field (magnetoplasmons) differs in frequency and the dispersion characteristics from conventional SPP.⁹ The magnetic field shifts the frequency of magnetoplasmon by changing the dielectric tensor of the medium. On the other hand, a plasmon resonance influences the magneto-optical properties of the system. The application of magnetic field to a plasmonic crystal allows new features in its magneto-optical response – e.g. in transversal and longitudinal magneto-optical Kerr effect (MOKE) – near the spectral and angular ranges of magnetoplasmons resonant excitation and the plasmonic band gap.^{10,11} The characteristic lifetime of SPP belongs to the range of about 100 fs. A femtosecond laser pulse interacting with such a short-living excitation gets coherently modified. Therefore, magnetoplasmons can demonstrate specific temporal magneto-optical response when having been excited by femtosecond laser pulse.^{12,13}

In this paper, we review our recent and new results in experimental observation of the resonant magneto-optical response in magnetoplasmonic crystals based on nanostructured magnetic metals, such as nickel and iron. We have shown that external quasistatic magnetic field can be used to control dispersion of SPP in magnetized metallic media. This leads to strong variation of magneto-optical effects, such as transverse and longitudinal magneto-optical Kerr effect. We also proposed a new approach of femtosecond intrapulse control of magneto-optical response by surface plasmon excitation.

Further author information: Send correspondence to A.A. Fedyanin: E-mail: fedyanin@nanolab.phys.msu.ru, Telephone: +7 495 939 4544

2. PHENOMENOLOGICAL MODEL

In the presence of external magnetic field SPP's have properties of magnetoplasmons.¹⁴ Let us consider the Faraday configuration which relates to the Voigt configuration of magnetoplasmons. In that case SPP can be expressed as a coherent superposition of two components $k_{spp}^{\circ,\circ}$ with right and left conical polarisations, correspondingly. Using linear approximation of g , dispersion relation for these components can be written as

$$k_{spp}^{\circ,\circ} = k_{spp} \left(1 \pm \frac{1}{2} \frac{\varepsilon_0}{(\varepsilon_0 + \varepsilon_1) \varepsilon_1} g \right), \quad (1)$$

where

$$k_{spp} = \frac{\omega}{c} \sqrt{\frac{\varepsilon_0 \varepsilon_1}{\varepsilon_0 + \varepsilon_1}} \quad (2)$$

is the SPP wavevector in the absence of magnetization, ε_0 is the dielectric permittivity of the space outside the magnetoplasmonic crystal, ε_1 is the diagonal component of the metal dielectric permittivity, and g is the magnitude of the gyration vector. The resulting SPP is obtained as the superposition of components $k_{spp}^{\circ,\circ}$ and the SPP polarisation is determined by the phase shift between them. The phase difference defines the enhancement of Kerr rotation (longitudinal MOKE) in the specular reflection.

In the second case suppose an external magnetic field is oriented along the boundary perpendicular to the SPP wavevector, as in the Voigt configuration. The magnetic field breaks the inverse symmetry in the plane of incidence, and therefore affects the value of wavevectors of propagating surface magnetoplasmons, which have opposite directions:

$$k_{SPP}^{\pm} = \pm k_{SPP} \frac{g \varepsilon_0}{\sqrt{-\varepsilon_0 \varepsilon_1 (\varepsilon_1^2 - \varepsilon_0^2)}}, \quad (3)$$

where g is the magnitude of the gyration vector. Induced inequality of these two vectors can be observed by the shift $\Delta\lambda$ of the resonance wavelength in the transverse magneto-optical Kerr effect (TMOKE)spectrum. The TMOKE value is $\delta = (R(H) - R(-H))/R_0$, where $R(H)$, $R(-H)$ and R_0 are reflectance with and without external magnetic field.

To calculate the effect in the 1D magnetoplasmonic crystal we use Fano-shape for reflection spectrum:¹⁵

$$|R(\omega)|^2 = |C_0 + \frac{f\Gamma e^{i\phi}}{\omega - \omega_0(H) + i\Gamma}|^2, \quad (4)$$

where C_0 is the non-resonant contribution rising due to specularly reflected light, f and ϕ are the strength and relative phase of the oscillator, $\omega_0(H)$ is the magnetic field-dependent central frequency of the SPP resonance, and Γ is the damping constant. The decay time of the SPP is defined as $\tau_{SPP} = 2/\Gamma$.

The ultrafast plasmonic response is determined by the lifetime of the surface plasmon. Let a magnetoplasmonic crystal with the spectrum $R(\omega)$ reflect a light pulse with Gaussian amplitude $E_G(t)$. The resulting amplitude of reflected pulse $E(t, 0)$ is a following convolution¹⁶:

$$E(t, H) = \int_{-\infty}^{+\infty} E_G(t') \times \left(f\Gamma e^{i\phi - (i\omega_0(H) + \Gamma)(t-t')} h(t-t') + C_0 \delta(t-t') \right) dt', \quad (5)$$

where $h(t)$ is the Heaviside step function and $\delta(t)$ is the Dirac delta function.

For numerical calculations we used SPP lifetime of $\tau_{SPP} = 30$ fs and resonance wavelength of $\lambda_0 = 1540$ nm, $\phi = -0.3\pi$, $C_0 = 0.7$, $f = 0.3$. The calculated reflection spectrum is shown in Fig.1(left). The local minimum at 1550 nm is described by energy transfer to the propagating SPP. For modeling of pulsed light reflection from magnetoplasmonic crystal we have set pulse duration $t_0 = 200$ fs and carrier wavelength $\lambda = 1560$ nm. In the presence of magnetic field the incident electric field $E(t, 0)$ becomes modified into $E(t, H)$ with the shift of the resonance wavelength estimated to be $\Delta\lambda \approx 0.4$ nm. Fig. 1(right) shows the normalized amplitude of reflected pulse and the normalized intensity difference $\Delta I(t) = |E(t, 0)|^2 - |E(t, H)|^2$.

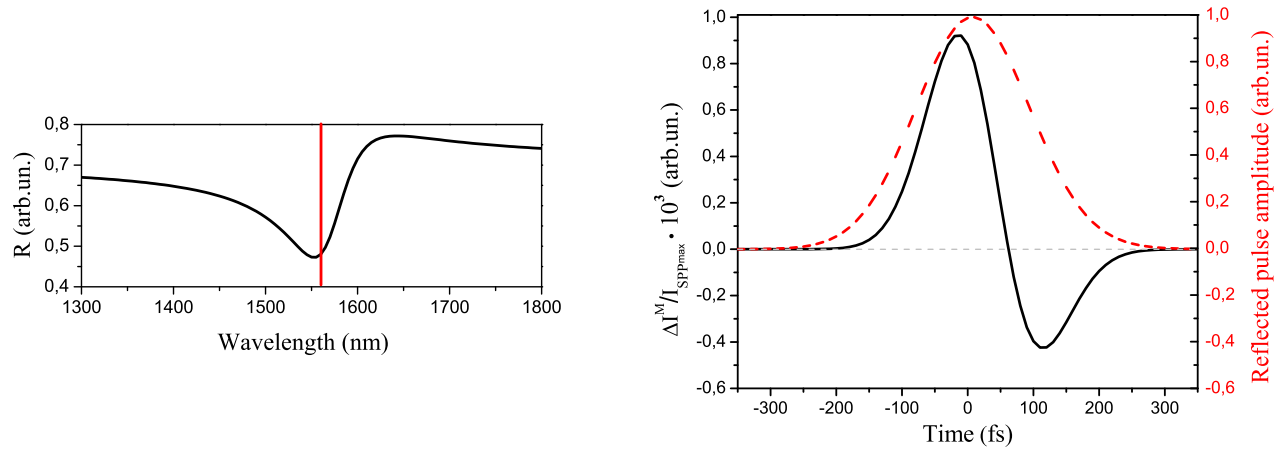


Figure 1. (left) Calculated reflectance spectrum of magnetoplasmonic crystal with the Fano resonance lineshape. Vertical line denotes the laser pulse central wavelength $\lambda = 1560$ nm used in numerical calculations. (right) Dashed curve – calculated normalized intensity $I(t, 0)$ of the pulse reflected from a magnetoplasmonic crystal without magnetic field. Solid curve – calculated magnetic field-induced intensity difference $\Delta I(t)$ normalized to the maximal value of $I(t, 0)$.

3. SAMPLES AND METHODS

For steady-state magnetoplasmonics we have used both 1D and 2D magnetoplasmonic crystals, for ultrafast magnetoplasmonics – 1D magnetoplasmonic crystal with different period. A 2D magnetoplasmonic crystal is realized as a hexagonal lattice of nickel nanodiscs on a 500- μm -thick nickel foil.¹⁰ The lattice period is 400 nm, the nanodisc diameter is 200 nm and its height is 50 nm.

1D magnetoplasmonic crystals were based on a 1D polymer subwavelength diffraction grating made by the nanoimprint lithography, where 100-nm-thick nickel film was further deposited by the thermal evaporation. The modulation depth of 1D sample is 50 nm. The sample period of 320 nm was used for steady-state experiments, and the sample period of 1500 nm – for ultrafast experiments. Fig. 4(a,b) show reflectance spectra of the 1D sample with the period of 1500 nm measured for the p-polarized light near normal incidence. Two parabolic-like stripes with low reflectance correspond with two plasmonic branches in band structure. At $\lambda \simeq 1530$ nm two plasmonic branches flow together, which specifies the presence of the plasmonic band gap. Fig. 4(a) shows the cross-section of reflection spectra for incident light angle $\theta \simeq 2^\circ$, which was chosen for ultrafast measurements. The reflectance spectrum has two minimums indicating the spectral position of SPP phase-matching using ± 1 st diffraction orders.

Plasmon-induced pulse shape switching under magnetization was observed by using a second harmonic generation intensity correlation setup based on a 130 mW Er^{3+} fiber infrared laser generating 200 fs pulses, for details see Ref. ¹⁶ The laser beam was split into two beamlets: a signal channel where the pulse was reflected from the 1D magnetoplasmonic sample and a reference channel with variable delay line. Both beamlets were then focused at a BBO crystal where the noncollinear second harmonic was generated when the pulses overlapped in time. The relatively small laser intensity allowed one to neglect nonlinear processes in metal such as laser-induced demagnetization.

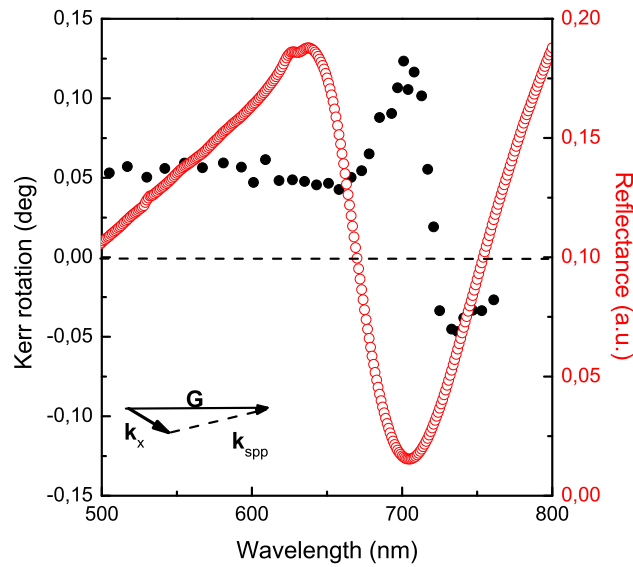


Figure 2. Kerr rotation (filled circles) and reflectance (open circles) spectra measured in 2D magnetoplasmonic crystal with angle of incidence of 45° . Inset: SPP phase-matching triangle.

4. STEADY-STATE MAGNETOPLASMONICS

Figure 2 shows experimental longitudinal Kerr rotation θ_K spectrum of 2D magnetoplasmonic crystal at the light incident angle of 45° in the 3-kOe saturated magnetic field. The phase matching triangle at the Wood's anomaly is shown in Fig. 2, where k_x is projection of the light wave vector onto the sample surface. The dip in the reflectance spectra for p-polarized light indicates the Wood's anomaly at 700 nm. The longitudinal MOKE θ_K is enhanced up to 0.15° at 700 nm. The effect changes the sign in the vicinity of the Wood' anomaly.

The experimental situation of longitudinal MOKE is realizing the Faraday configuration of magnetoplasmonic modes excitation. In this case plasmonic wave contains a TE component as well and SPP can be represented as a coherent superposition of two components with right and left conical polarizations. Total amplitude of SPP is determined by the coherent superposition of these components and the SPP polarization is determined by the phase shift between them. Then, the phase difference controls the enhancement of Kerr rotation obtained in the specular direction.

Figure 3 shows experimental of TMOKE and reflectance spectra for the 1D magnetoplasmonic crystal at the light incident angle of 60° for two azimuthal orientations of reciprocal vector \mathbf{G} with respect to the incident plane. The curve in Fig. 3 is a reflectance spectrum for p-polarized light measured in specular direction as reciprocal vector \mathbf{G} is oriented within the plane of incidence providing the phase-matching conditions for effective SPP excitation. The dip in the reflectance spectra for p-polarized light indicates the Wood's anomaly at 615 nm. The TMOKE spectrum is shown in Fig. 3 by open circles has a resonant Fano-type feature and changes the sign in the vicinity of the Wood' anomaly. The reference TMOKE spectrum shown by open circles is measured for the sample azimuthal orientation as reciprocal vector is perpendicular to the incident plane providing absence of effective SPP excitation due to the phase-matching conditions. The spectrum monotonously decreases with the wavelength without any resonances just as a plain nickel surface.

Enhancement of transverse MOKE is interpreted as a result of the SPP dispersion curve shift upon the magnetization reversal at the surface of magnetoplasmonic crystal. Since the value of transversal MOKE is proportional to the reflectivity difference for opposite magnetization directions, the spectral dependence of transversal MOKE has an asymmetric resonant lineshape. In this way transverse MOKE relates to the Voigt configuration of magnetoplasmons, where surface magnetoplasmon modes become asymmetric with respect to the magnetization direction and the dispersion spectrum reveals a magnetic-field-induced shift. Polarization of magnetoplasmon

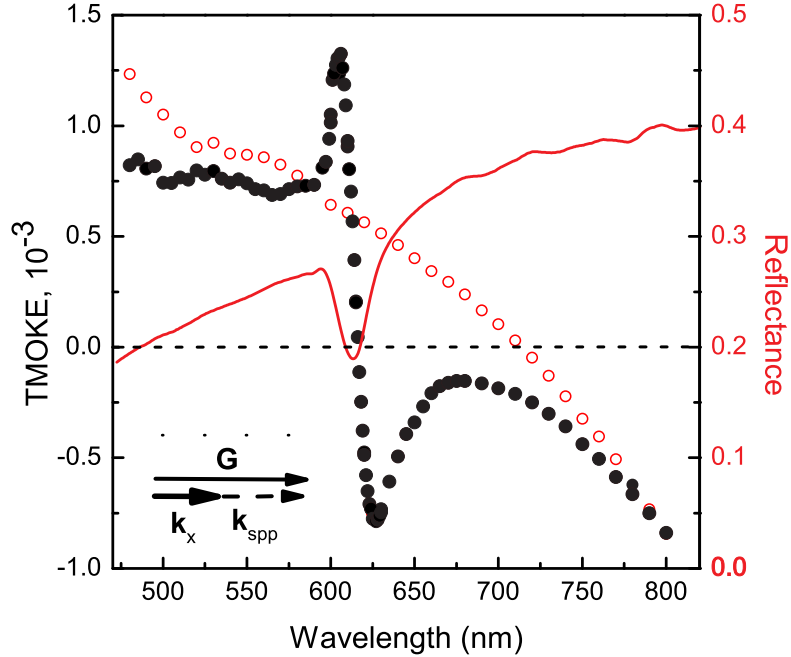


Figure 3. TMOKE (filled circles) and reflectance (curve) spectra of 1D magnetoplasmonic crystal with angle of incidence of 60° for reciprocal vector oriented within the plane of light incidence. Open circles denote TMOKE spectrum of 1D magnetoplasmonic crystal with reciprocal vector perpendicular to the plane of incidence. Inset: SPP phase-matching triangle.

wave remains to be TM just as in the absence of magnetic field, while the wavevector of magnetoplasmonic mode depends on the value of the off-diagonal component of dielectric permittivity.

5. ULTRAFAST MAGNETOPLASMONICS

In ultrafast measurements intensity correlation scheme with second harmonic generation has been used. The photodetector measures the correlation function I_{CF} of pulse intensity $I(t, H)$ reflected from the 1D magnetoplasmonic crystal:

$$I_{CF}(\tau) = \int_{-\infty}^{+\infty} I_G(\tau - t') I(t', H) dt', \quad (6)$$

where $I_G(t)$ – intensity of reference pulse, τ – the time delay between the laser pulses.

After applying an alternating magnetic field and measuring signal locked-in to its frequency one can detect the variation ΔI_{CF} of correlation function:

$$\Delta I_{CF}(\tau) = \int_{-\infty}^{+\infty} I_G(\tau - t') ((I(t', H) - I(t', -H)) dt'. \quad (7)$$

Fig. 4(c) shows correlation function $I_{CF}(\tau)$ and $\Delta I_{CF}(\tau)$ measured for the p -polarized light. The correlation function $I_{CF}(\tau)$ was measured for zero magnetic field and shows no difference in the lineshape from the autocorrelation function of the laser. This result is expected as the pulse duration is several times longer than the SPP lifetime in nickel. The correlation function variation $\Delta I_{CF}(\tau)$ was measured in the presence of 300-Oe external magnetic field alternating with the frequency of 115 Hz. The latter was applied to the sample perpendicularly to the plane of incidence, corresponding to the Voigt configuration for SPP propagation.

$\Delta I_{CF}(\tau)$ is positive within the interval from -200 fs to 20 fs with the maximum at $\tau = -50$ fs, and negative between 20 fs to 300 fs with the minimum at $\tau = 100$ fs. The absolute value of the maximum exceeds the absolute value of the minimum, which was predicted by the numerical calculations shown in Fig. 1(right). From this it

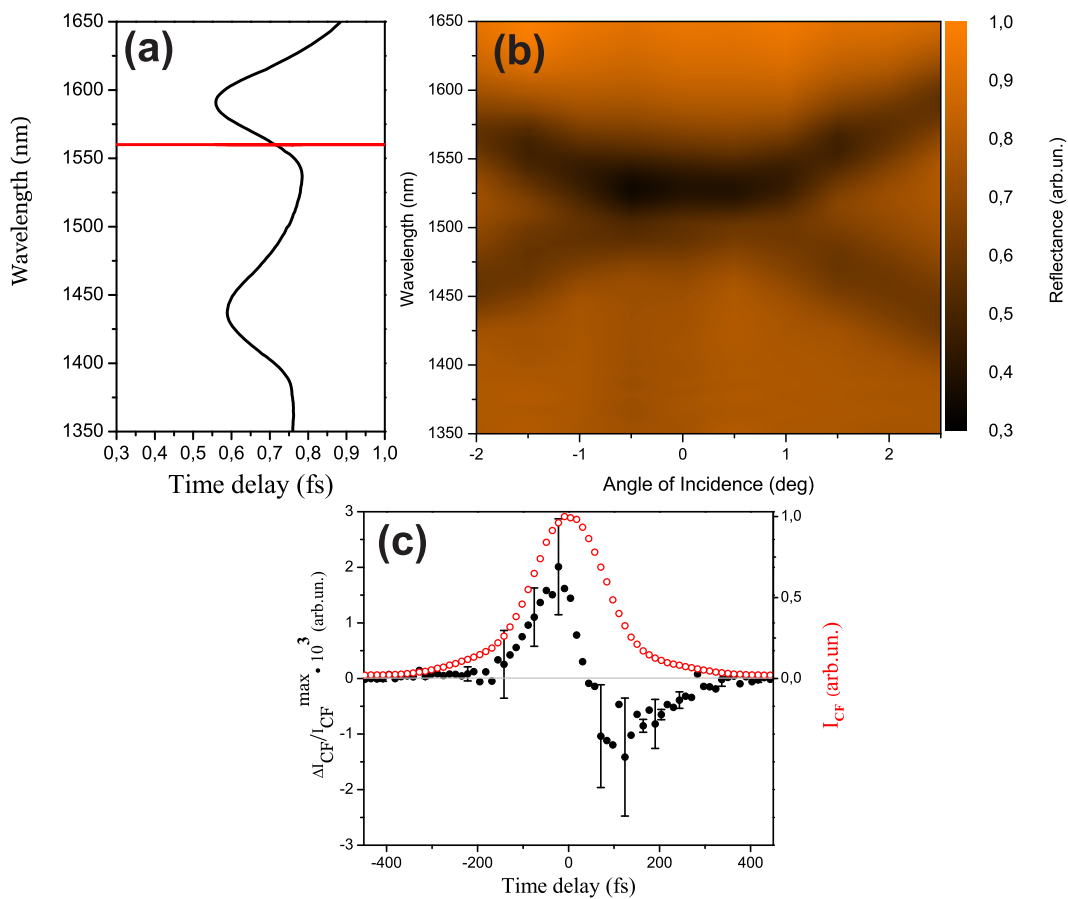


Figure 4. (a) Measured reflectance spectrum of 1D magnetoplasmonic crystal for incident angle $\theta \approx 2^\circ$. Vertical line denotes the laser pulse central wavelength $\lambda = 1560$ nm used in time-resolved measurements. (b) Experimental reflectance of the magnetoplasmonic crystal sample as a function of wavelength λ and angle of incidence θ for the p -polarized incident light. (c) Measured normalized correlation function I_{CF} (open circles) and normalized to the maximal value of I_{CF} correlation function variation $\Delta I_{CF}(t)$ (filled circles) measured at the frequency of external magnetic field for the p -polarized incident laser pulse with duration $t_0 = 200$ fs reflected from magnetoplasmonic crystal.

follows that the SPP-induced ultrafast pulse switching has been confirmed by the experiment. Magnetic field shifts the SPP resonance wavelength, which affects in the shaping of the reflected pulses and, consequently, variation of the correlation function. In our recent paper¹³ it was shown that the value of time-dependent magnetisation-induced $\Delta I_{CF}(\tau)$ is significantly higher in 1D iron-based magnetoplasmonic crystal.

6. CONCLUSIONS

In conclusion, resonant magneto-optical response was shown in magnetoplasmonic crystals. Longitudinal and transverse MOKE are enhanced in the vicinity of Wood's anomaly. We demonstrated experimentally and numerically femtosecond magnetic field-induced shaping of femtosecond laser pulses reflected from 1D magnetoplasmonic crystal. The effect of the SPP-induced ultrafast pulse switching is explained by the resonance wavelength shift caused by magnetic field application. The given results show a promising pathway for ultrafast laser pulse manipulation by magnetoplasmonic structures.

ACKNOWLEDGMENTS

The work was supported by Russian Ministry of Education and Science (project ID RFMEFI61314X0029).

REFERENCES

1. Wurtz, G.A., Hendren, W., Pollard, R., Atkinson, R., Le Guyader, L., Kirilyuk, A., Rasing, Th., Smolyaninov, I.I., Zayats, A.V., "Controlling optical transmission through magneto-plasmonic crystals with an external magnetic field," *New J. Phys.* 10, 105012 (2008).
2. Khurgin, J. B., "Optical isolating action in surface plasmon polaritons," *Appl. Phys. Lett.* 89, 251115 (2006).
3. Grunin, A.A., Zhdanov, A.G., Ezhov, A.A., Ganshina, E.A., Fedyanin, A.A., "Surface-plasmon-induced enhancement of magneto-optical Kerr effect in all-nickel subwavelength nanogratings", *Appl. Phys. Lett.* 97, 261908 (2010).
4. Armelles, G., Cebollada, A., Garcia-Martin, A., & Gonzalez, M.U. , "Magnetoplasmonics: combining magnetic and plasmonic functionalities," *Advanced Optical Materials* 1, 10-35 (2013).
5. Barnes, W. L., Dereux, A., & Ebbesen, T. W., "Surface plasmon subwavelength optics," *Nature* 424, 824-830 (2003).
6. Garcia-Vidal, F.J., Martin-Moreno L., "Transmission and focusing of light in one-dimensional periodically nanostructured metals," *Phys. Rev. B* 66, 155412 (2002).
7. Porto, J.A., Garcia-Vidal, F.J., Pendry, J.B., "Transmission resonances on metallic gratings with very narrow slits," *Phys. Rev. Lett.* 83, 2845 (1999).
8. Barnes, W.L., Preist, T.W., Kitson, S.C., Sambles, J.R., "Physical origin of photonic energy gaps in the propagation of surface plasmons on gratings," *Phys. Rev. B* ;54, 6227 (1996).
9. Chiu, K.W., and Quinn, J.J., "Magnetoplasma surface waves in metals," *Phys. Rev. B* 5, 4707 (1972).
10. Chetvertukhin, A.V., Grunin, A.A., Baryshev, A.V., Dolgova, T.V., Uchida, H., Inoue, M., Fedyanin, A.A., "Magneto-optical Kerr effect enhancement at the Wood's anomaly in magnetoplasmonic crystals", *J. Magn. Magn. Mater.* 324, 3516 (2012).
11. Chetvertukhin, A.V., Grunin, A.A., Dolgova, T.V., Inoue, M., Fedyanin, A.A., "Transversal magneto-optical Kerr effect in two-dimensional nickel magnetoplasmonic crystals", *J. Appl. Phys* 113, 17A942 (2013).
12. Vabishchevich, P.P., Frolov, A.Yu., Shcherbakov, M.R., Grunin, A.A., Dolgova, T.V., Fedyanin, A.A., "Magnetic field-controlled femtosecond pulse shaping by magnetoplasmonic crystals", *J. Appl. Phys.* 113, 17A947 (2013).
13. Shcherbakov, M.R., Vabishchevich, P.P., Frolov, A.Yu., Dolgova, T.V., Fedyanin, A.A., "Femtosecond intrapulse evolution of the magneto-optic Kerr effect in magnetoplasmonic crystals", *Phys. Rev. B.* 90, 201405 (2014).
14. Brion, J. J., Wallis, R. F., Hartstein, A., & Burstein, E., "Theory of surface magnetoplasmons in semiconductors", *Phys. Rev. Lett.* 28, 1455 (1972).
15. Ropers, C., Park, D. J., Stibenz, G., Steinmeyer, G., Kim, J., Kim, D. S., & Lienau, C., "Femtosecond light transmission and subradiant damping in plasmonic crystals", *Phys. Rev. Lett.* 94, 113901 (2005).
16. Vabishchevich, P. P., Bessonov, V. O., Sychev, F. Y., Shcherbakov, M. R., Dolgova, T. V., & Fedyanin, A. A., "Femtosecond relaxation dynamics of surface plasmon-polaritons in the vicinity of fano-type resonance", *JETP Lett.* 92, 575 (2010).